cosmetics

MDPI

Article

Bio-Functional Investigation and AI-Driven Target Interaction Prediction of Chrono Control Penta as a Plant Multifunctional Dermo Cosmetic Peptide

Carmen Lammi [1,*], Raffaele Pugliese [2], Lorenza d'Adduzio [1], Umberto Maria Musazzi [1], Gilda Aiello [3], Melissa Fanzaga [1], Maria Silvia Musco [1] and Carlotta Bollati [1]

[1] Department of Pharmaceutical Sciences, University of Milan, 20133 Milan, Italy
[2] Plantech s.r.l., 20133 Milan, Italy
[3] Department of Human Science and Quality of Life Promotion, Telematic University San Raffaele, 00166 Rome, Italy
* Correspondence: carmen.lammi@unimi.it

Abstract

Skin aging is influenced by both internal and external factors, resulting in wrinkles, decreased elasticity and irregular pigmentation. Hyaluronic acid (HA), a key component of the extracellular matrix, is essential for skin hydration and structural support. Peptides, short amino acid chains, have gained attention in cosmetics due to their multifunctional biological activities. This study explored the moisturizing and metal-chelating properties of Chrono Control Penta (S-Cannabis Sativa-pentapeptide-1), a novel plant-derived peptide whose sequence is WVSPL. In vitro, it chelated iron ions up to 17.86 ± 2.50% and copper ions up to 47.08 ± 1.49% at 10 mM and 3 mM, respectively. Western blot and Enzyme-Linked Immunosorbent Assay (ELISA) analysis showed that, under H_2O_2-induced stress, Chrono Control Penta increased hyaluronan synthase 2 (HAS2) production by 81.72% in BJ-5ta fibroblasts and enhanced HA secretion by 20.11% compared to simulated aging conditions alone, respectively. Furthermore, experiments carried out with the Franz diffusion cell and human full thickness skin demonstrated the peptide's ability to penetrate the skin layers and even diffuse laterally with a quantified peptide skin biodistribution accounting for 0.095/0.06 nM/mg in 6 h. Advanced AI-based modeling (AlphaFold2, RosettaFold) and docking analysis revealed stable peptide-peptide transporter 2 (PEPT2) interactions, supporting carrier-mediated skin permeation and linking computational predictions with experimental diffusion data. Hence, this study extends previous evidence on the cosmetic efficacy of Chrono Control Penta by (i) adding mechanistic insights into metal chelation and HAS2/HA modulation, (ii) rigorously quantifying local skin penetration and lateral diffusion with HPLC-MS/MS, and (iii) providing a plausible mechanistic link between skin biodistribution and PEPT2-mediated transport based on deep learning structural models.

Keywords: Chrono Control Penta; skin aging; skin permeability; cosmetic peptides

check for updates

Academic Editor: Enzo Berardesca

Received: 16 October 2025
Revised: 18 November 2025
Accepted: 22 November 2025
Published: 27 November 2025

Citation: Lammi, C.; Pugliese, R.; d'Adduzio, L.; Musazzi, U.M.; Aiello, G.; Fanzaga, M.; Musco, M.S.; Bollati, C. Bio-Functional Investigation and AI-Driven Target Interaction Prediction of Chrono Control Penta as a Plant Multifunctional Dermo Cosmetic Peptide. *Cosmetics* **2025**, *12*, 267. https://doi.org/10.3390/cosmetics12060267

Copyright: © 2025 by the authors. Licensee MDPI, Basel, Switzerland. This article is an open access article distributed under the terms and conditions of the Creative Commons Attribution (CC BY) license (https://creativecommons.org/licenses/by/4.0/).

1. Introduction

Peptides have become fundamental in the cosmetic sector because of their precise targeting, compatibility with biological systems and wide range of biological functions which they are able to exert [1].

As short chains of amino acids (2–20), they have been shown to play key roles in physiological processes such as signaling, repair and molecular regulation, and these

distinctive properties make them essential for addressing challenges ranging from chronic diseases to skin health promotion [2]. Notably, their generally low skin barrier permeability may restrict delivery and efficacy [3].

In this context, our research group has recently demonstrated the multi-functionality of Chrono Control Penta (WVSPL), a novel and patented bioactive peptide, commercially available (https://www.plantechlab.com/, accessed on 24 November 2025), which is able to promote beneficial effects both in vitro and on human skin [4]. Chrono Control Penta exemplifies the importance of combining innovative cosmetic solutions with safer and more sustainable synthetic strategies, minimizing both reliance on potentially harmful substances such as trifluoroacetic acid (TFA) and the use of chemical modification at N- and/or C-terminus, with the aim of improving peptide stability (acetylation/amidation) or skin permeability (fatty acid conjugation).

Furthermore, previous research provided evidence of Chrono Control Penta's safety and efficacy, reporting its anti-aging, anti-pigmentation, moisturizing and anti-pollution properties, demonstrated both in vitro by using biochemical techniques and cellular models, particularly skin fibroblasts and melanocyte cell lines and in vivo in human volunteers [4].

Building upon these findings, the present study aims to further characterize the Chrono Control Penta profile, extending the scope of its biological evaluation for deepening both its safety and efficacy in cosmetic performance.

Therefore, first, an in vitro skin permeation study was conducted using the Franz diffusion cell and human full thickness skin as a membrane to evaluate the safety of Chrono Control Penta, excluding its ability to reach the systemic circulation, in agreement with Regulation (EC) No. 1223/2009 on cosmetic products and Commission Implementing Decision 2013/674/EU, which highlight that avoiding systemic exposure is a fundamental requirement for cosmetic ingredients http://data.europa.eu/eli/dec_impl/2013/674/oj (accessed on 10 October 2025). In parallel, the same experimental technique was used to measure the peptide's ability to penetrate the skin layers and even diffuse laterally, a crucial feature for its biological activity and cosmetic efficacy. Moreover, the present work reveals novel biological activities and the related mechanism of action of the pentapeptide that can scientifically explain the beneficial multifunctional cosmetic effects that were observed in vivo on human volunteers [4]. Specifically, peptide's metal-chelating ability was assessed using in vitro assays. In addition, we aimed to investigate the potential molecular mechanism underlying the moisturizing bioactivity exerted by Chrono Control Penta, by evaluating its ability to modulate the hyaluronan synthase 2 (HAS2) expression in human fibroblasts.

Finally, to deepen our understanding of its structural and mechanistic behavior, we employed advanced AI-based protein modeling and molecular docking analyses for explaining its skin bioavailability.

Together, these computational and experimental outcomes offer a comprehensive view of Chrono Control Penta's bioactivity, confirming its local action, structural stability and receptor-mediated interaction potential, key features supporting its inclusion in next-generation dermo-cosmetic formulations. Hence, the novelty of the study relies on demonstrating an integrated bio-functional and delivery profile, combining metal chelation, induction of HAS2/HA, and confirmed skin biodistribution, while directly correlating AI-based transporter binding predictions with empirical permeation data to establish a mechanistic link between molecular results and topical efficacy already validated in human study [4].

2. Materials and Methods

2.1. Chemicals

All chemicals and reagents employed in this study were of analytical grade and commercially obtainable. RIPA buffer, protease inhibitor cocktail, PMSF, sodium orthovanadate, Pyrocatechol Violet (P7884), Iron(II) chloride (98%), 3-(2-Pyridyl)-5,6-diphenyl-1,2,4-triazine-p,p′-disulfonic acid monosodium salt hydrate, Copper(II) sulfate pentahydrate, bovine serum albumin (BSA), Ethylenediaminetetraacetic acid (EDTA) and the β-actin antibody were obtained from Sigma-Aldrich (St. Louis, MO, USA). Dulbecco's Modified Eagle's Medium (DMEM), L-glutamine, fetal bovine serum (FBS), phosphate-buffered saline (PBS), penicillin/streptomycin, chemiluminescent substrate, dry milk powder, and multi-well plates were sourced from Euroclone (Milan, Italy). Mini-PROTEAN TGX precast 7.5% gels and Mini Nitrocellulose Transfer Packs were purchased from Bio-Rad (Hercules, CA, USA). The Human Hyaluronic Acid (HA) ELISA Kit (Catalog No. CSB-E04805h) was supplied by Cusabio (Wuhan, China). Rabbit Ig-HRP and mouse Ig-HRP secondary antibodies were purchased from Santa Cruz Biotechnology, Inc. (Santa Cruz, CA, USA). Antibody targeting Hyaluronan synthase 2 (HAS2 antibody) was obtained from Proteintech (Rosemont, IL, USA).

2.2. Evaluation of Chrono Control Penta Iron Metal Chelation

The Iron-chelating activity of the peptide was evaluated using a colorimetric ferrozine-based assay as reported by Wong et al. with slight modifications [5]. In detail, the assay was conducted in 1.5 mL microcentrifuge tubes and reactions included 10× peptide solution (25 µL) or vehicle (only H_2O), 125 µL of sterile filtered H_2O, and 11 µL of $FeCl_2$ (1 mM final concentration). Chrono Control Penta was tested at the final concentrations of 0.001, 0.01, 0.1, 1.0, and 10.0 mM. Ethylenediaminetetraacetic acid (EDTA) at 0.05% w/v concentration, corresponding to 1.3 mM, was used as positive control. All were incubated for 2 min, then 100 µL of ferrozine was added to each tube (0.5 mM final concentration) and left for 10 min. Then, 80 µL of the reaction mixture was aliquoted in triplicate into a transparent 96-well plate and the absorbance was measured at 562 nm by using a microplate reader Synergy H1 (Agilent Biotek, 20063 Cernusco sul Naviglio (MI), Italy). A red control (only vehicle) indicated full Fe^{2+}-ferrozine complex formation, while reduced color intensity indicated metal chelation by the peptide or EDTA. The metal chelating activity (%) was determined according to the following equation:

$$\%\ Iron\ Chelation = 1 - \left(\frac{Abs\ sample}{Abs\ control} \times 100\right)$$

2.3. Evaluation of Chrono Control Penta Copper Metal Chelation

For carrying out the copper-chelation assay, we followed the procedure reported by Yap et al. [6]. In particular, a 50 mM sodium acetate buffer at pH 6.0 was prepared, along with a 4 mM pyrocatechol solution and a copper solution at a concentration of 1 mg/mL in sterile filtered H_2O. For each reaction, 280 µL of sodium acetate buffer, 10 µL of the copper solution, and 10 µL of the peptide (30× concentration of peptide solution) or vehicle (only H_2O) were mixed in 1.5 mL microcentrifuge tubes to reach the final concentrations of 0.3, 1.0, 2.0, and 3.0 mM, respectively. After 2 min incubation at room temperature, 6 µL of 4 mM pyrocatechol solution was added for each experimental condition. Then, 100 µL of the reaction mixture was aliquoted in triplicate into a transparent 96-well plate and the absorbance was measured at 632 nm using a microplate reader Synergy H1 (Agilent Biotek, 20063 Cernusco sul Naviglio (MI)). Ethylenediaminetetraacetic acid (EDTA) at 0.05% w/v

concentration, corresponding to 1.3 mM, was used as positive control. The percentage of copper chelating activity was calculated as follows:

$$\%\ Copper\ Chelation = \frac{Abs\ control - Abs\ sample}{Abs\ control} \times 100$$

2.4. Cell Culture Condition

The hTERT-immortalized human skin fibroblast cell line BJ-5ta (ATCC® CRL-4001™, obtained from LGC Standards, Milan, Italy) was cultured in a 4:1 mixture of high-glucose DMEM and Medium 199, supplemented with stable L-glutamine, 10% fetal bovine serum (FBS), 100 U/mL penicillin, and 100 µg/mL streptomycin. Cells were maintained at 37 °C in a humidified atmosphere with 5% CO_2.

2.5. Hyaluronan Synthase 2 (HAS2) Protein Level Evaluation with Western Blot Experiments

BJ-5ta hTERT-immortalized human skin fibroblasts were seeded at a density of 1.8×10^5 cells per well in 12-well plates and maintained at 37 °C in a humidified atmosphere with 5% CO_2. After 24 h, cells were treated with 50 µM Chrono Control Penta or vehicle (H_2O) in complete growth medium for an additional 24 h. The following day, cells were exposed to 0.2 mM hydrogen peroxide (H_2O_2) overnight to mimic aging-related conditions, or with vehicle. After treatments, supernatants were collected to be further analyzed with Enzyme-Linked Immunosorbent Assays (ELISAs), while cells lysates were then collected by scraping in 40 µL of ice-cold lysis buffer [RIPA buffer supplemented with protease inhibitor cocktail, PMSF (1:100), and sodium orthovanadate (1:100)], and transferred to pre-chilled microcentrifuge tubes. Lysates were centrifuged at 13.300× *g* for 15 min at 4 °C, and the supernatants were transferred to fresh ice-cold tubes. Total protein concentration was determined using the Bradford assay, and 50 µg of protein per sample was run and separated on a precast 7.5% SDS-polyacrylamide gel (SDS-PAGE) at 120 V for 60 min. Proteins were transferred to nitrocellulose membranes (Mini Nitrocellulose Transfer Packs, Bio-Rad) using a Trans-Blot Turbo system (Bio-Rad) at 1.3 A, 25 V for 7 min. After blocking with either milk or BSA, membranes were probed with primary antibodies against Hyaluronan synthase 2 (HAS2) and β-actin. HRP-conjugated secondary antibodies and a chemiluminescent substrate were used for signal detection. Bands were visualized and quantified using Image Lab Software 6.1 version (Bio-Rad, Via Benvenuto Cellini, 18/A, 20090 Segrate (MI)). Protein expression levels were normalized to β-actin as an internal loading control.

2.6. Enzyme-Linked Immunosorbent Assays (ELISAs) for Hyaluronic Acid Quantification in Cell Culture Supernatants

The Human Hyaluronic Acid (HA) ELISA Kit by CUSABIO (Via Ranzato, 20128 Milano) was used to measure hyaluronic acid levels in cell culture supernatants. Experiments were carried out following the manufacturer's instructions. Samples (100 µL) were added to each well and incubated for 2 h at 37 °C. After removal of the liquid, 100 µL of biotinylated antibody (1×) was added to each well, which were then incubated for 1 h at 37 °C, followed by three washes with wash buffer. HRP-avidin (1×, 100 µL) was then added to each well and incubated for 1 h at 37 °C, after which wells were washed five times with wash buffer. The substrate solution (TMB, 90 µL) was added and the reaction developed for 10–20 min at 37 °C in the dark. The reaction was then stopped with 50 µL of stop solution, and, subsequently, the absorbance was measured at 450 nm within 5 min by using the Synergy H1 plate reader (Agilent Biotek, 20063 Cernusco sul Naviglio (MI)). The percentage of hyaluronic acid detected in the supernatants of treated cells was compared to that measured in untreated control cells, which were set as 100%.

2.7. In Vitro Skin Permeation Study

The permeation study was performed by using Franz diffusion cells (diffusion area: 0.636 cm^2; receptor volume: ≈3.0 mL) and human full thickness skin from Caucasian donors as a membrane. The human epidermis originated from the abdominal skin of a donor who underwent cosmetic surgery. The full thickness skin was sealed in evacuated plastic bags and stored within 6 h after removal. The integrity of skin specimens was visually checked before the experiments. At the beginning of the permeation experiment, the skin specimen was mounted on the receiver compartment of the Franz diffusion cell, whose receptor compartment was filled with sterile 0.9% sodium chloride aqueous solution (Fresenius Kabi, Italy). Particular care was given to avoid air bubbles between the solution and the skin in the receptor compartment. The upper and lower parts of the Franz cell were sealed with Parafilm® (Pechiney Plastic Packaging Company, Stamford, CT, USA) and fastened together by means of a clamp, with the skin specimen acting as a seal between the donor and receptor compartments. The system was kept at 35 °C with a circulating water bath to the skin surface temperature at 32 °C throughout the experiment. At time zero, the tested formulation was applied on the stratum corneum of each skin sample. In particular, 0.5 mL of Chrono Control Penta solution, (tested at the same concentration of the in vivo study, corresponding to 0.5%, *w*/*v*) was loaded directly in the donor compartment of each cell. At predetermined times (1, 3, 6 h), 200 µL samples were withdrawn from the receiver compartment and replaced with fresh receiver medium. Samples were analyzed by HPLC-MS/MS according to the method described below. The values were the average of parallel experiments performed in triplicate. The cumulative amount permeated through the human skin per unit area ($Q_{t,\ perm}$) was calculated from the peptide concentration in the receiving medium and plotted as a function of time [7]. At the end of the permeation experiments, the concentration of Chrono Control Penta retained in the full-thickness skin ($Q_{6h,\ ret}$) was quantified by the HPLC-MS/MS technique. The skin specimen was removed from the Franz diffusion cell and stripped (Transpore®, 3M, St. Charles, MO, USA) to eliminate the unabsorbed formulation. Then, each side of the membrane was gently treated with 5 mL of purified H_2O to wash out the unabsorbed peptide. Subsequently, skin was lysed following the methods described in the section below.

2.8. Skin Lysis

Each skin sample from the Franz diffusion chamber was cut on a clean glass plate using a fine scalpel to accurately separate the central area (LC) from the lateral area (LL), as the lateral area contains the percentage of diffused peptide, while the central area contains the percentage of peptide directly absorbed. The skin was lysed using 3.0 mm Zirconium beads for 4 min at maximum speed (BeadBug™ homogenizer, Benchmark Scientific, Sayreville, NJ, USA) using a ratio of 300 µL of lysis buffer (6 M urea in 50 mM Tris/50 mM NaCl buffer, pH 8) per 80 mg of skin. The lysate was then collected and centrifuged at 14.000 rpm for 20 min at 4 °C, and the supernatants were collected. A 3 kDa cut-off filtration was then performed for the supernatants (13.500 rpm, 20 min, 4 °C), with the aim to concentrate the peptides absorbed in the skin to be further analyzed.

2.9. HPLC-MS/MS Analysis for the Quantification of the Absorbed Chrono Control Penta in the Skin and in the Basolateral Solutions of the Franz Diffusion Cells

All samples have been analyzed at UNITECH OMICs (University of Milan, Italy) using Agilent 1290 Infinity II LC (Agilent, 20063 Cernusco sul Naviglio (MI)) connected to an Agilent 6495 LC/TQ (Agilent).

Chromatographic separation was achieved on a ZORBAX ECLIPSE PLUS C18 (Agilent) 50 mm (Length) × 2.1 mm (ID) × 1.8 µm (Particle Size) using mobile phase A (water with

formic acid 0.1%) and mobile phase B (acetonitrile with formic acid 0.1%) at a flow rate of 400 µL/min. The elution program was set as follows: 0–2 min 10% B; 2–17 min from 10 to 70% B; 17–18 min from 70 to 90% B; 18–19 min 90% B; 19–20 min from 90 → to 10% B; 20 min 10% B. The column and autosampler temperatures were set at 40 °C and 15 °C, respectively.

MS spectra were acquired using electrospray ionization in positive mode (+ESI), operating in Multiple Reaction Monitoring (MRM). Transitions were optimized for each analyte, and retention times (tRs) were determined under the chromatographic conditions described above. The quantification of Chrono Control Penta peptide (WVSPL) was performed by monitoring the transitions that included the parent ion $(M+H)^+$ at m/z 601.3 with the following product ions: m/z 229.2 (quantifier), m/z 316.2 (qualifier), and m/z 258.2 (qualifier), all with a retention time of 5.5 min.

2.10. In Silico Tools for Chrono Control Penta Structure Prediction

2.10.1. Peptide Selection and Input Preparation

The Chrono Control Penta peptide sequence WVSPL was selected as a representative short peptide to assess the predictive accuracy of two state-of-the-art deep learning models for protein structure prediction: AlphaFold2 [8] and RosettaFold [9]. The sequence was formatted in standard FASTA notation and used as the sole input for all prediction runs. No experimental templates or homologous structures were provided to ensure a fully de novo prediction scenario. Similarly, no secondary structure restraints were imposed, allowing both algorithms to infer peptide folding exclusively from learned statistical patterns and evolutionary signals.

2.10.2. AlphaFold2 Prediction Protocol

Structural prediction using AlphaFold2 was performed through the AlphaFold v2.3 pipeline with all five pretrained neural network models (Models 1–5). The following settings were applied to ensure high reproducibility: (1) input (WVSPL in FASTA format); (2) recycles per model (0–6 iterations); (3) template use (disabled, template-free mode); (4) multiple sequence alignment (MSA), generated using HHblits and JackHMMER searches against UniRef90 and MGnify databases; (5) relaxation step, performed with the Amber energy minimization protocol. For each model and recycle iteration, AlphaFold2 automatically produced key performance metrics: (1) predicted local distance difference test (pLDDT) to measure residue-level confidence (0–100 scale); (2) predicted TM-score (pTM) to estimate the accuracy of global fold topology; (3) RMSD tolerance, which measures deviation across recycling cycles. The best-performing model was selected based on the highest pLDDT and lowest RMSD tolerance. Structural visualization and validation were conducted using PyMOL v2.5 and UCSF ChimeraX v1.5.

2.10.3. RosettaFold Prediction Protocol

Parallel predictions were conducted using RosettaFold, an integrated three-track neural network developed by the Baker laboratory. The same peptide sequence (i.e., WVSPL) was provided as input, following a comparable template-free strategy, using: (1) input (WVSPL in FASTA format); (2) recycling iterations (0–6 iterations); (3) template use (disabled, template-free mode); (4) multiple sequence alignment (MSA), generated using HH-search pipeline against BFD and UniRef90; (5) relaxation step, executed through the Rosetta energy minimization protocol. Each output model was evaluated using: (1) pLDDT; (2) predicted alignment error (PAE) to estimate the inter-residue positional uncertainty; (3) RMSD tolerance. Performance trends were extracted from JSON output files and analyzed to quantify model convergence behavior and refinement consistency over successive recycling steps.

2.10.4. Model Confidence and Structural Accuracy Metrics

The pLDDT score represents the model's confidence in the local atomic arrangement of each residue. Scores above 70 are generally considered reliable for backbone regions, while values below 50 may indicate flexible or disordered segments. The pTM score (AlphaFold2) estimates the global topological accuracy of the model, while PAE (RosettaFold) quantifies the positional uncertainty between residue pairs. Together, these metrics describe the global structural consistency and alignment accuracy of the predicted models. RMSD was computed across recycling steps to assess structural convergence and refinement. Lower RMSD values indicate higher model stability and accuracy. For AlphaFold2, RMSD tolerance values were derived from internal model outputs, while for RosettaFold, RMSD was calculated via PyMOL's rms_cur command after backbone alignment. Structural superimpositions were performed in PyMOL and ChimeraX to compare the top-ranked AlphaFold2 and RosettaFold models. Quantitative analyses focused on residue-wise pLDDT comparison between the two prediction systems, global RMSD and PAE/pTM evaluations, and visual inspection of fold consistency, side-chain packing, and terminal region variability. All numeric and graphical analyses were conducted in Python 3.10 using the Matplotlib and NumPy libraries.

2.11. Statistical Analysis

All data are presented as mean ± standard deviation (s.d.) of at least three biological independent experiments. Each of them were conducted at least in duplicates or triplicates. A p-value < 0.05 was considered statistically significant. Statistical analyses were carried out using one-way ANOVA followed by Tukey's post hoc test, and Brown–Forsythe test was used for checking the homogeneity of variance (GraphPad Prism 10, GraphPad Software, La Jolla, CA, USA).

3. Results

3.1. Dual Iron and Copper Chelating Activity by Chrono Control Penta

Metal ions, such as copper and iron, possess unpaired electrons and act as key catalysts in Fenton-type reactions; by binding these ions, metal-chelating peptides can inhibit free radical generation [10]. Moreover, the role of copper-binding peptides in skin regeneration, antioxidant activity, and tyrosinase inhibition has been well-established [11,12] while it is known that metal chelation may help protect and maintain hair health as well [13]. Considering this knowledge, Chrono Control Penta demonstrated measurable and dose-dependent iron and copper chelating activities, respectively. As reported in Figure 1a, data clearly show that Chrono Control Penta was able to chelate iron in a tested concentration range between 0.001 and 10 mM. In particular, it was able to chelate iron by 3.13 ± 1.0%, 4.77 ± 0.75%, 7.27 ± 1.36%, 12.19 ± 2.06%, and 17.86 ± 2.50%, at the final concentrations of 0.001, 0.01, 0.1, 1.0, and 10.0 mM, respectively, while EDTA 0.05% w/v, which was used as the positive control condition, was able to chelate iron by 87.3 ± 0.24%.

In addition, data reported in Figure 1b demonstrate the dose-dependent ability of Chrono Control Penta to chelate copper ions in a tested concentration range between 0.3 and 3 mM. In detail, Chrono Control Penta could chelate copper ions by 14.71 ± 4.56%, 24.21 ± 1.85%, 35.14 ± 2.35%, and 47.08 ± 1.49% at the final tested doses of 0.3, 1.0, 2.0, and 3.0 mM, respectively. Additionally, EDTA 0.05% w/v, which was used as the positive control condition, could chelate copper by 94.9 ± 3.1%.

Thus, results clearly suggest that Chrono Control Penta is more potent in chelating copper than iron. Indeed, it can chelate copper about 30 times more efficiently than iron at 1 mM (Figure 1). This significant copper-chelating activity adds to peptide's multiple known biological properties; in contrast, EDTA, although showing a higher chelating

efficacy, is typically included in cosmetic formulations for its stabilizing and preservative functions and does not possess any intrinsic biological activity.

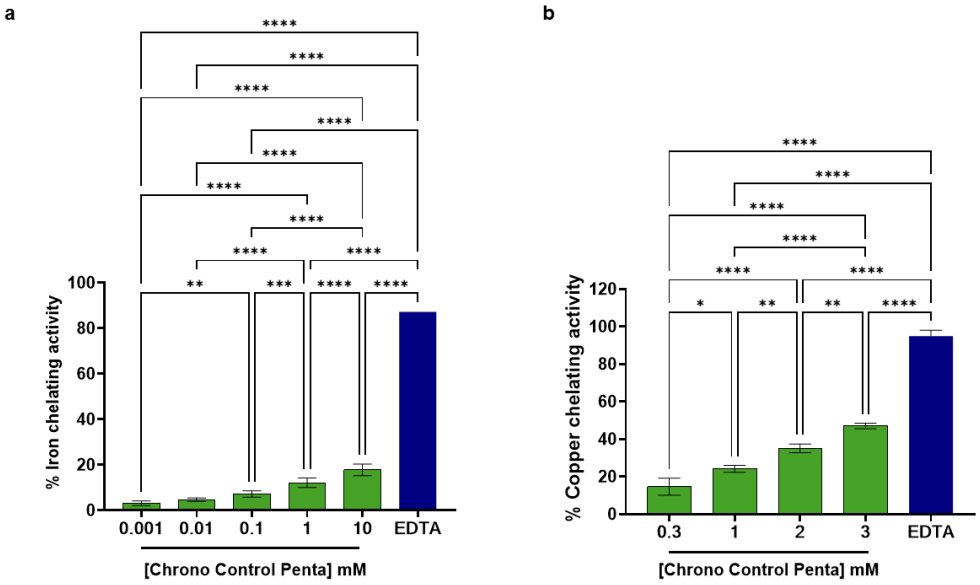

Figure 1. In vitro Effects of Chrono Control Penta on Iron (**a**) and Copper (**b**) Chelation. Data represents the mean ± s.d. of three independent experiments performed in triplicate. * ($p < 0.05$), *** ($p < 0.001$), ** ($p < 0.01$), **** ($p < 0.0001$), not statistically significant comparisons are not shown.

3.2. Chrono Control Penta Improves the Synthesis of Hyaluronan Synthase 2 (HAS2) in Aged Human Skin Fibroblasts

In our previous work, we demonstrated that Chrono Control Penta is safe at the cellular level in BJ-5ta human skin fibroblasts, as confirmed by viability assays [5]. Furthermore, we showed its ability to significantly counteract skin-aging processes both in vitro, at the active concentration of 50 µM, and in vivo, in a study on volunteers. In the latter, Chrono Control Penta (0.5% *w*/*v*) was well tolerated and was found to gradually lighten the skin, reduce wrinkles, improve dermal firmness, exert a purifying effect, and enhance skin hydration, with a measured moisturizing effect of 9.17% after 15 days and 13.05% after 6 weeks [4].

Notably, collagen and hyaluronic acid (HA) are essential for skin structure and hydration, but with the aging process, HA synthesis, regulated by hyaluronan synthase 2 (HAS2), declines and thus leads to dryness, loss of elasticity, and wrinkles; therefore, maintaining HAS2 activity is crucial to counteract skin aging [14].

Considering this evidence, our results clearly show that under simulated aging conditions, reproduced by treating H_2O_2 at 200 µM concentration [4], the HAS2 protein levels significantly decreased by 23.39 ± 8.16% compared with untreated control cells. Notably, the treatment with Chrono Control Penta counteracted this aging effect, restoring and even enhancing HAS2 production. Indeed, at a concentration of 50 µM, the peptide increased HAS2 levels to 139.3 ± 24.21% relative to untreated controls, which corresponds to an 81.72% increase compared to H_2O_2 conditions in dermal fibroblasts (Figure 2). The increase in HAS2 protein levels is comparable to that observed following treatment with collagen peptides, which were used as a positive control, as collagen peptides have been shown to enhance HAS2 expression up to 135.4 ± 23.7% relative to untreated cells, which corresponds to 76.7% augmentation compared to aging conditions.

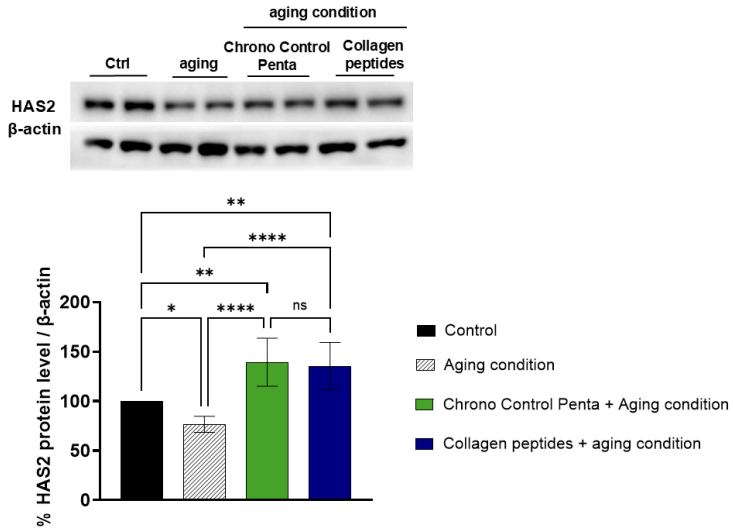

Figure 2. Effects of Chrono Control Penta on HAS2 production in human skin fibroblasts. Cells were pre-treated with 50 μM Chrono Control Penta for 24 h, or with collagen peptides at 5 mg/mL concentration, after which aging conditions were induced with H_2O_2 overnight. Data represents the mean ± s.d. of six independent experiments performed in duplicate. Ctrl: not stimulated and not treated cells; Aging c.: cells treated with H_2O_2. * ($p < 0.05$), ** ($p < 0.01$), **** ($p < 0.0001$), ns: not significant.

3.3. Enhancement of Hyaluronic Acid (HA) Secretion by Chrono Control Penta in Aged Human Skin Fibroblasts Assessed via Enzyme-Linked Immunosorbent (ELISA) Assay

Chrono Control Penta was shown to significantly enhance HAS2 expression in cultured fibroblasts, leading us to subsequently evaluate its effect on HA secretion, a key process in preserving skin hydration and elasticity under pro-aging stress conditions.

Indeed, we exploited an ELISA, conducted on human dermal cells supernatants, to measure the functional levels of HA secreted by H_2O_2-stressed cells and to evaluate the ability of Chrono Control Penta to positively modulate HA production in simulated pro-aging stress conditions at the cellular level.

As reported in Figure 3, under H_2O_2 stress, HA secretion decreased by 18.16 ± 9.75% compared to untreated control cells, while pre-treatment with Chrono Control Penta at the final concentration of 50 μM significantly restored HA production to 97.77 ± 15.51%.

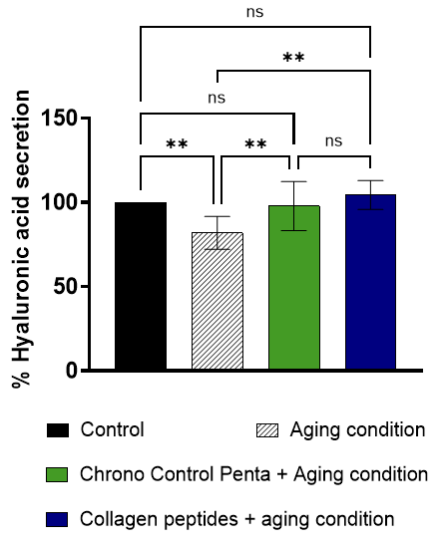

Figure 3. Effects of Chrono Control Penta on HA secretion in human skin fibroblasts. Cells were pre-treated with 50 μM Chrono Control Penta for 24 h, or with collagen peptides at 5 mg/mL concentration, after which aging conditions were induced. Data represents the mean ± s.d. of four

independent experiments performed in triplicate. Control: not stimulated and not treated cells; Aging c.: cells treated with H_2O_2. ** ($p < 0.01$), ns: not significant.

Data thus reveal that Chrono Control Penta was able to enhance HA secretion by 20.11% compared to aging conditions in human fibroblasts; this result is in line with the HAS2 production and this effect is comparable to that observed with collagen peptides treatment ($p < 0.05$). All these molecular and functional results can explain the moisturizing effect and cellular hydration observed in vivo after already 15 days [4].

3.4. In Vitro Skin Permeability of Chrono Control Penta Assessed by Franz Diffusion Cell and Human Full Thickness Skin and Quantified via HPLC-MS/MS

The skin, the largest organ of the human body, is composed of multiple layers with distinct cellular compositions, including the epidermis and the underlying dermis [15]. In our previous study, we demonstrated in vivo, in human volunteers, that Chrono Control Penta exerts various beneficial biological effects for the skin [5]. In the present study, we further evaluated its skin permeability by using the Franz diffusion cell and human full thickness skin as membrane approach, thus analyzing the entire skin samples after their lysis with a dedicated lysis buffer described above, to quantify both the absorbed and laterally diffused fractions of the peptide. Quantification was performed using HPLC/MS-MS in MRM mode (transitions 601.3 → 229.2, 316.2, 258.2), providing a quantitative and detailed assessment of peptide penetration and distribution in the tissue.

The calibration curve was linear over the concentration range 31.25–1000 nM with the regression equation y = 632.85x + 300.49 and R^2 = 0.9985. The method exhibited excellent precision (CV% = 0.42–14.54), and accuracy was approximately 90%. The limit of detection (LOD) and limit of quantification (LOQ), calculated as 3.3σ/S and 10σ/S from the lowest calibration point, were 10.9 nM and 33.2 nM, respectively.

After incubation (6 h), measurable Chrono Control Penta levels were detected both in the lysed skin tissue (LC, 47 ± 17.6 nM) and in the laterally diffused fraction (LL, 63 ± 47.3 nM). When normalized to the skin mass, these values correspond to 0.045 ± 0.02 nM/mg and 0.05 ± 0.04 nM/mg for LC and LL, respectively (Table 1). In addition, Chrono Control Penta was not detected in the receptor compartment, and the cumulative permeated amount ($Q_{t,\ perm}$) was below the detection limit (LOD = 10.9 nM).

Table 1. Quantification of peptide Chrono Control Penta (nM) after incubation in Franz diffusion cells normalized against the mg of skin (LC and LL). Concentrations [nM/mg] measured by HPLC–MS/MS in central skin lysates (LC) and laterally diffused fractions (LL) are shown as mean ± s.d. of three independent experiments performed in triplicate.

Skin Lysates	[nM/mg]
central skin lysates (LC)	0.045 ± 0.02
laterally diffused fractions (LL)	0.05 ± 0.04

When expressed as a percentage of the initial Chrono Control Penta concentration incubated in Franz diffusion cells, the peptide recovery in the skin lysate accounted for ~0.001%. The slightly higher amount recovered in the lateral diffusion compartment suggests that the peptide can spread through the skin layers. This lateral movement could be due to peptide surface affinity with the skin layer.

The detection of Chrono Control Penta within the epidermal and dermal compartments, in the absence of measurable amounts in the receptor phase, indicates that the peptide is bioavailable to skin cells while remaining locally confined. Such a profile is consistent with topical bioactivity and negligible systemic exposure. Small peptide re-

tention within skin tissue layers can favor interaction with keratinocytes and fibroblasts, supporting local biological effects while minimizing systemic diffusion and potential off-target exposure.

3.5. Structure Prediction Performance of AlphaFold2 and RosettaFold

To assess the predictive accuracy and confidence of deep learning models for Chrono Control Penta peptide, it was modeled using AlphaFold2 and RosettaFold under identical template-free conditions (see Materials and Methods for further details). Both tools generated multiple models across successive recycling iterations to improve prediction confidence and structural refinement. Model quality was evaluated using pLDDT, RMSD, and global confidence metrics (pTM for AlphaFold2, PAE for RosettaFold). Despite employing distinct neural network architectures and training paradigms, both methods successfully converged on compact, stable structures for the peptide, though with marked differences in convergence rate, local confidence, and stability (Figure 4a–e).

AlphaFold2 produced high-confidence structures for Chrono Control Penta from the first prediction cycle. Across the five model configurations, model 3 consistently achieved the highest local confidence scores, with pLDDT values ranging from 0.765 at the initial cycle to 0.757 after two recycles, indicating stable predictions even with minimal recycling (Figure 4a). The pTM-score remained stable between 0.042 and 0.046, suggesting that the global fold topology was preserved throughout the prediction process (Figure 4b). AlphaFold2's RMSD tolerance values were minimal, reaching 0.141 Å after two recycles, reflecting rapid structural convergence and minimal deviation between predicted states (Figure 4c).

Instead, RosettaFold exhibited a more gradual improvement in structure quality across recycling iterations, consistent with its stepwise refinement architecture (Figure 4a). The pLDDT scores increased from 0.499 (recycle 0) to 0.690 (recycle 6), indicating a steady enhancement in per-residue confidence through successive refinement cycles. The PAE values decreased from 9.594 to 5.633, denoting improved inter-residue positioning and global fold consistency (Figure 4b). Likewise, the RMSD dropped sharply from 10.051 Å at recycle 0 to 1.190 Å at recycle 6, demonstrating significant convergence toward a stable structure (Figure 4c). However, mild fluctuations in RMSD were observed between cycles 4 and 5, suggesting temporary instability during later optimization stages. Despite these variations, RosettaFold ultimately achieved a compact, physically plausible structure with moderate local confidence and reduced global error.

Overall, the comparative performance of the two models revealed consistent trends in predictive capability and convergence behavior (Table 2). AlphaFold2 consistently produced higher confidence scores and lower RMSD values, achieving accurate predictions with minimal recycles. Its stable pTM scores and minimal RMSD tolerance highlight its efficiency and precision, especially in capturing compact secondary structures. RosettaFold, while initially less accurate, displayed a clear trajectory of improvement, progressively reducing both PAE and RMSD with each recycle. This iterative refinement behavior underscores the strength of RosettaFold's three-track network, which integrates sequence, distance, and coordinate representations to incrementally improve model geometry.

Next, the visual inspection of the predicted models corroborated the quantitative metrics (Figure 4d,e). The AlphaFold2 structure exhibited uniformly high pLDDT coloration (blue–cyan, 75–85 range) across the backbone, signifying consistent confidence throughout the peptide chain (Figure 4d). Correspondingly, the PAE heatmap displayed low predicted alignment errors across all residue pairs, confirming stable intra-chain relationships. By contrast, RosettaFold generated a model with mixed confidence regions, displaying green-to-yellow coloration (pLDDT ~0.6–0.7), particularly at the terminal residues (Figure 4e).

The associated PAE plot showed localized zones of higher uncertainty, suggesting partial flexibility or limited residue–residue constraint resolution in these regions. Despite these local discrepancies, both methods produced comparable global folds, supporting the validity of their predictions and highlighting complementary modeling behaviors—rapid confidence stabilization in AlphaFold2 versus gradual refinement in RosettaFold.

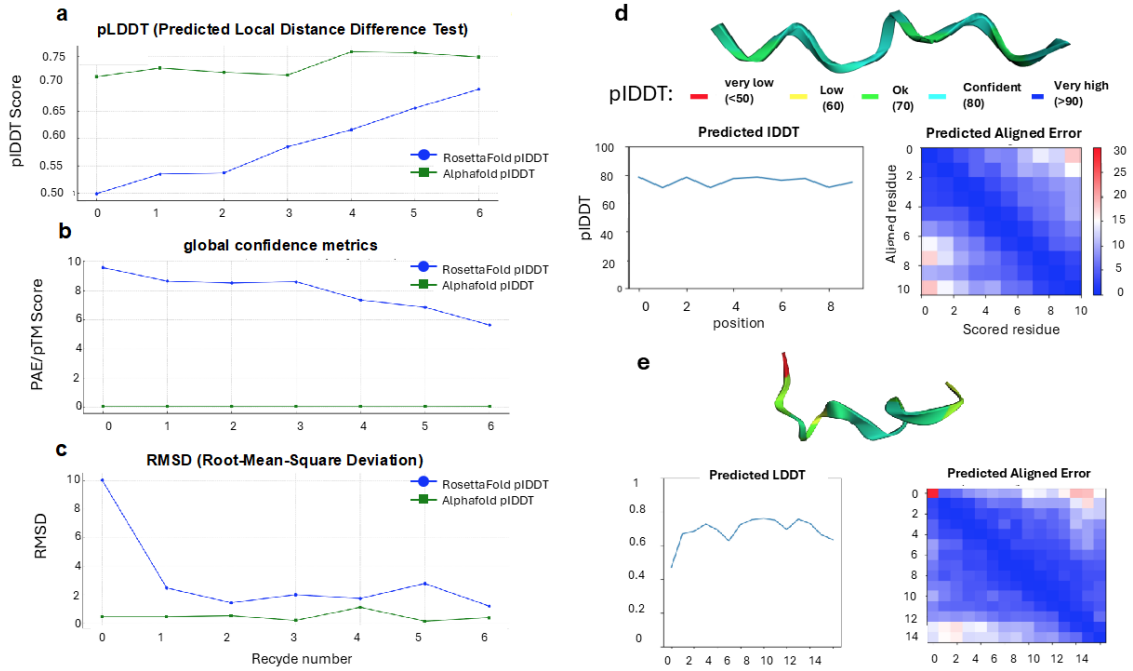

Figure 4. Comparative assessment of Chrono Control Penta peptide structure predictions by AlphaFold2 and RosettaFold. Chrono Control Penta was modeled under identical template-free conditions using both deep learning approaches. (**a**) Per-residue confidence (pLDDT) across successive recycling iterations shows that AlphaFold2 rapidly achieves high-confidence predictions, while RosettaFold gradually improves local confidence. (**b**) Global fold metrics (pTM for AlphaFold2, PAE for RosettaFold) indicate stable topology for AlphaFold2 from the first cycle and progressive refinement for RosettaFold. (**c**) RMSD values reflect rapid structural convergence for AlphaFold2 and stepwise convergence for RosettaFold, with minor fluctuations in later cycles. (**d**) AlphaFold2 models display uniformly high per-residue confidence (pLDDT 0.75–0.85, blue–cyan) across the backbone, with low PAE, indicating consistent structural reliability and stable intra-chain relationships. (**e**) RosettaFold models show heterogeneous confidence (pLDDT ~0.6–0.7, green–yellow), especially at terminal residues, with localized PAE elevations reflecting partial flexibility or less constrained residue-residue interactions. Despite local variations, both methods generate comparable global folds, illustrating complementary modeling behaviors: rapid confidence stabilization in AlphaFold2 versus progressive refinement in RosettaFold.

Table 2. Comparative analysis of AlphaFold2 and RosettaFold.

Metric	AlphaFold2	RosettaFold
Initial pLDDT	0.713	0.499
Final pLDDT	0.759	0.690
pTM/PAE	0.042–0.046	9.594–5.633
RMSD final	0.141–1.105 Å	1.190 Å
Recycles to convergence	1–2	5–6

Such observed differences can be attributed to architectural and training distinctions between the models. AlphaFold2's transformer-based attention modules allow effective encoding of long-range residue interactions, even in short sequences, facilitating rapid

convergence and stable local confidence. Conversely, RosettaFold's three-track architecture, which alternates between sequence, distance, and coordinate representations, emphasizes iterative correction of geometric features, leading to gradual but consistent refinement across recycles. For short peptides such as Chrono Control Penta, the limited sequence context may favor AlphaFold2's attention-driven learning, enabling it to infer local geometry directly from intrinsic statistical correlations. RosettaFold, in contrast, may benefit more from longer input sequences, where its integrated refinement process can exploit richer MSA information.

To validate the computational predictions, circular dichroism (CD) spectroscopy was performed on the synthesized Chrono Control Penta peptide to experimentally assess its secondary structure in aqueous solution (Supplementary Figure S1). The CD spectrum exhibited a characteristic negative band near 200 nm and a broad shoulder around 220 nm, indicative of a predominantly disordered or turn-rich conformation with partial β-structure tendencies. These spectral features closely mirrored the secondary structure content predicted by AlphaFold2, which suggested a compact backbone with limited regular secondary elements and moderate flexibility at the termini. The strong correspondence between the experimental CD profile and the AlphaFold2-predicted conformation supports the accuracy and physical plausibility of the computational fold, confirming that the deep learning model captured the peptide's intrinsic structural tendencies under near-physiological conditions.

3.6. Docking Analysis of the Predicted Chrono Control Penta Peptide with PEPT2 and Implications for Skin Permeation

Following the structural prediction phase, the AlphaFold2-derived conformation of the Chrono Control Penta peptide was utilized for molecular docking studies to investigate its potential interaction with the human peptide transporter PEPT2 [16]. PEPT2 is a proton-coupled oligopeptide transporter primarily expressed in epithelial tissues, including the skin, where it facilitates the uptake of di- and tripeptide-like molecules. Given its physiological relevance in peptide transport and drug permeation, the docking analysis aimed to elucidate whether Chrono Control Penta could serve as a potential substrate or modulator of PEPT2-mediated transport mechanisms.

The optimized AlphaFold2 structure of Chrono Control Penta, characterized by high local confidence (pLDDT $\approx$ 0.76) and low RMSD, was used as input for docking simulations. The receptor model of PEPT2 was obtained from the Protein Data Bank (PDB ID: 7NQK). The results revealed a stable and specific interaction between WVSPL and the catalytic site of PEPT2, with the peptide occupying the canonical substrate-binding groove. Notably, hydrogen bonding was observed between the peptide's tryptophan (W), proline (P), and serine (S) residues and the receptor's site residues Tyrosine634, Lysine161, and Serine626 (Figure 5). The predicted binding affinity was consistent with that of known PEPT2 substrates, such as LRP, GPA, and WWW peptides (Supplementary Figure S2), suggesting favorable compatibility. In particular, the interface predicted TM-score (ipTM), a confidence metric used to evaluate the accuracy of predicted interfaces between protein chains within a complex, indicated high reliability, with values of 0.86, 0.88, 0.78, and 0.80 for the Chrono Control Penta, LRP, GPA, and WWW peptides, respectively. These findings indicate that the AlphaFold2-predicted structure of WVSPL adopts a conformation suitable for recognition by PEPT2, potentially enabling facilitated transport across epithelial barriers such as the skin. The observed docking pattern supports the hypothesis that small peptides with amphiphilic and aromatic residues may exploit PEPT2-mediated pathways to enhance transdermal permeation. Furthermore, the peptide's compact and stable conformation predicted by AlphaFold2 appears critical for its favorable binding orientation within the catalytic cavity.

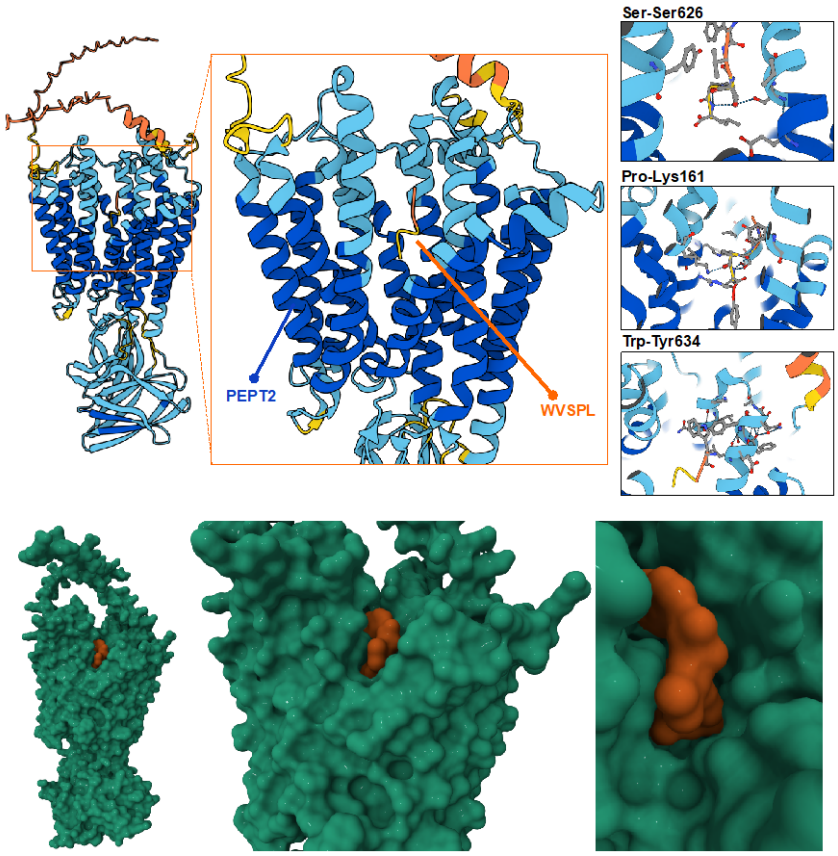

Figure 5. Molecular docking analysis of the AlphaFold2-optimized Chrono Control Penta peptide with the PEPT2 receptor. The high-confidence Chrono Control Penta structure predicted by AlphaFold2 was docked into the catalytic site of PEPT2. The peptide occupies the substrate-binding groove, forming stable hydrogen bonds between WVSPL residues Trp, Pro, and Ser and receptor residues Tyr634, Lys161, and Ser626. The docking pose indicates strong spatial complementarity and a binding affinity consistent with known PEPT2 substrates. Moreover, in the bottom of the figure, the molecular surface configuration shows the substrate binding groove Chrono Contral Penta (in orange) and PEPT2 (in green).

From a translational standpoint, this result suggests that computationally predicted peptide structures can guide the rational design of bioactive or transport-enhancing sequences for topical and transdermal delivery applications. The integration of deep learning-based structure prediction with docking simulations thus provides a powerful framework for elucidating structure–function relationships in peptide–transporter systems and for identifying promising candidates for skin-permeation-enhancing formulations.

4. Discussion

Skin health results from a complex interaction between hydration, oxidative balance, firmness, and protection against external factors such as ultraviolet (UV) radiation and pollution [17,18]. Recent findings highlight that aging is not merely chronological but is also strongly influenced by extrinsic stressors [19]. A central factor in maintaining skin elasticity and barrier integrity is hyaluronic acid (HA), a polysaccharide abundant in the dermis and upper epidermal layers, responsible for water retention, osmotic balance, and tissue stability [20].

Among bioactive ingredients, peptides have emerged as multifunctional cosmetic agents able to modulate various biological pathways involved in skin aging, hydration, and regeneration [21]. They can be classified into four main categories: signal, carrier, neurotransmitter-inhibitory, and enzyme-inhibitory peptides [22]. Signal peptides mimic

natural molecular messengers that activate fibroblasts and promote the synthesis of extracellular matrix (ECM) proteins, such as collagen, elastin, and glycosaminoglycans [23]. Well-known examples include Palmitoyl pentapeptide-4 (Matrixyl®), which enhances collagen production and reduces wrinkle depth; Tripeptide-10 Citrulline (Decorinyl®), which mimics decorin to stabilize collagen fibrils; and Palmitoyl tripeptide-5 (Syn®-Coll), which upregulates transforming growth factor-beta (TGF-β) to boost skin elasticity. Carrier peptides like Copper tripeptide-1 (Cu-GHK) and Manganese tripeptide-1 (Mn-GHK) deliver essential metal ions that support enzymatic activities and structural integrity. Acetyl hexapeptide-3 (Argireline®), a neurotransmitter-inhibitory peptide, reduces dynamic wrinkles by modulating SNARE complex formation, offering botulinum toxin-like effects with excellent safety [24–30].

Our recent research focuses on a novel peptide isolated from hempseed proteins, newly registered as S-Cannabis Sativa-pentapeptide-1 (Chrono Control Penta). This pentapeptide combines properties of both signal and enzyme-inhibitory peptides, exerting multifunctional cosmetic activity. Previous studies demonstrated its anti-aging and hydrating efficacy: the peptide significantly increased collagen (+87.5%), elastin (+61.3%), and secretion levels of these proteins, while reducing MMP-2 and MMP-9 expression in aged fibroblasts. Clinically, after six weeks of treatment with a cream containing 0.5% Chrono Control Penta, volunteers showed improved hydration (+13%), firmness (+6%), wrinkle reduction (+11.5%), and skin brightness (+12%), with no adverse reactions observed [4].

Importantly, the peptide also shows metal-chelating activity, binding Fe^{2+} and Cu^{2+} ions in a dose-dependent manner (Figure 1), even though with a different potency. More in detail, Chrono Control Penta is 30 times more efficient in chelating copper than iron at 1 mM. However, overall, the peptide's metal chelating property contributes to cell protection from metal-induced oxidative damage; in fact, chelating metal ions (like iron or copper) reduces the formation of highly reactive Fenton-type radicals, thereby protecting skin structures and function [31]. Additionally, this activity promotes anti-pigmentation effects observed in the volunteers, correlated in vitro with the tyrosinase inhibition and melanin production reduction in melanocytes, and with cosmetic formulation stability, limiting metal-catalyzed degradation [4]. Thus, our findings support the double ability of Chrono Control Penta to inhibit tyrosinase activity by both direct interaction (IC_{50} 202.8 μM [4]) and copper chelation, which is crucial for its enzymatic function [32]. These results are in accordance with those observed in vivo and represent a deeper characterization of its mechanism of action, explaining the beneficial cosmetic claims observed in the in vivo study.

Hence, at the molecular level, our new findings reveal that Chrono Control Penta enhances the expression of Hyaluronan Synthase 2 (HAS2) and boosts HA synthesis in human fibroblasts exposed to oxidative stress, demonstrating that the peptide not only protects against damage but actively stimulates HA biosynthesis, thereby improving skin hydration, elasticity, and structure (Figures 2 and 3).

Similarly to our results, Bang and colleagues recently discovered a novel peptide named Medipep, through a phage display biotechnological technique, which was able to increase collagen synthesis in skin cells (1.18-fold increase testing 1000 ppm of the peptide) and to upregulate the expression of the aquaporin-3 (AQP3) and HAS2 genes, while substantial reduction in wrinkles occurred after 6 weeks of treatment with the peptide in a clinical study conducted on 20 female volunteers with a mean age of 49.4 ± 5.08 years [33]; moreover, black rice hydrolyzed peptides from germinated Oryza sativa L. var. japonica significantly modulate gene expression in HaCaT keratinocytes, notably upregulating HAS2 and enhancing HA production in a dose-dependent manner [34].

Additionally, Zonari and colleagues reported a study where a 12-week clinical trial was designed to evaluate the effectiveness of a topical formulation containing the OS-01 peptide, demonstrating that, after 12 weeks of product use, trans epidermal water loss decreased by 17.33% and hydration increased by 32.49% [35]. In another study, Norzagaray-Valenzuela et al. demonstrated that peptides derived from three species of microalgae (*Dunaliella tertiolecta*, *Tetraselmis suecica*, and *Nannochloropsis* sp.) exert hyaluronidase inhibition in a species-dependent manner, with modest inhibition for *D. tertiolecta* (15.16%) and *T. suecica* (18.5%) at 0.9 μg/μL, and a stronger effect observed for *Nannochloropsis* sp. [36]; these results indicate that while microalgal peptides reduce HA degradation through hyaluronidase inhibition, Chrono Control Penta promotes HA synthesis via HAS2 modulation, illustrating how distinct peptides can act on complementary levels of the HA pathway, ultimately converging on the regulation of HA homeostasis.

In accordance, another study was carried out by Kim et al., showing that a low-molecular collagen peptide from fish scales promoted HA production in HaCaT keratinocytes, primarily by upregulating HAS2 expression and protein levels, while concurrently downregulating hyaluronidase 1 (HYAL1) to limit HA degradation, potentially acting as functional ingredient in moisturizing products [37].

Permeation and safety assessments were performed using the Franz diffusion cell and human full thickness skin as membrane system. Chrono Control Penta was not detected in the receptor chamber, confirming that it does not cross the full skin barrier and cannot reach systemic circulation, a key regulatory requirement for cosmetic ingredients under EU Regulation (EC) No. 1223/2009. Nonetheless, the peptide effectively penetrates and diffuses within the epidermal and dermal layers, reaching its target cells locally, ensuring efficacy without systemic exposure (Table 1). Indeed, although the peptide concentration measured in the ex vivo setup was low, this does not imply that such concentration is sufficient to reproduce the beneficial cosmetic effects observed in vivo. In addition, it is important to underline that the ex vivo investigation of skin permeability is an efficient and well-recognized model to assess the permeation ability of cosmetics, but at the same time, from a technical point of view, this system is less physiologically similar to live skin tissue. For example, in vivo, the skin's barrier function is influenced by a variety of intrinsic and extrinsic factors, including aging, hydration and environmental conditions, which can increase or decrease cosmetic molecule penetration [38]. In contrast, in ex vivo models, this dynamic nature may be lost, potentially resulting in different local cosmetic concentrations at the site of action. Therefore, the current ex vivo data should be interpreted as an indication of the basic permeation behavior of the peptide, and, not less importantly, as a safety indicator, rather than a direct explanation of in vivo performance. The previously reported clinical efficacy reflects the more complex physiological conditions of living skin, which include blood flow, dynamic barrier properties and formulation effects, which may enhance peptide delivery and activity.

Finally, to deepen our understanding of its structural and mechanistic behavior, advanced AI-based protein modeling and molecular docking analyses were employed. The structure prediction performance of AlphaFold2 and RosettaFold was systematically compared on the Chrono Control Penta (Table 2). AlphaFold2 demonstrated superior predictive confidence and rapid structural convergence, whereas RosettaFold exhibited gradual refinement over multiple recycling steps. This dual-model approach enabled a robust validation of the predicted conformation, highlighting AlphaFold's advantage in short peptide modeling while confirming RosettaFold's complementary interpretability (Table 2, Figure 4). The most stable conformation obtained from AlphaFold2 was subsequently employed for molecular docking analysis with the PEPT2 receptor, a proton-dependent oligopeptide co-transporter implicated in peptide translocation across epithelial tissues, where it

is clearly expressed (Figure 5) [39]. The results revealed favorable binding interactions between WVSPL and the PEPT2 catalytic site, suggesting that the peptide could exploit carrier-mediated pathways for localized skin permeation (Figure 5). Although Chrono Control Penta can potentially be transported via the PEPT2-mediated transport mechanism, we cannot exclude that some other route of passage, e.g., passive diffusion, may occur simultaneously in the skin. However, this insight provides a mechanistic explanation for the observed lateral diffusion within the epidermis and dermis, linking computational predictions to experimental findings.

5. Conclusions

In conclusion, Chrono Control Penta is a multifunctional and safe cosmetic peptide able to chelate metals, stimulate HAS2, and HA production, combined with excellent skin compatibility and non-systemic penetration. These results contribute to positioning it as a promising ingredient for next-generation dermo cosmetic formulations.

6. Patents

The authors declare that Patent WO2025114961A1, "Methods to counteract skin aging", is owned by Università degli Studi di Milano, which is directly related to the content of this publication. It has been licensed to Plantech s.r.l.

Supplementary Materials: The following supporting information can be downloaded at: https://www.mdpi.com/article/10.3390/cosmetics12060267/s1, Figure S1: CD spectrum of Chrono Control Penta; Figure S2: AlphaFold2 Molecular docking analysis.

Author Contributions: Conceptualization, C.L.; methodology, R.P., U.M.M. and C.B.; validation, C.B., G.A. and R.P.; formal analysis, R.P., C.B. and G.A.; investigation, C.B., M.S.M., L.d., U.M.M., G.A., R.P. and M.F.; data curation, R.P. and C.B.; writing—original draft preparation, M.F., G.A. and R.P.; writing—review and editing, R.P., C.L. and C.B.; supervision, C.L.; funding acquisition, C.L. All authors have read and agreed to the published version of the manuscript.

Funding: This research was partially funded by PLANTECH S.R.L.

Institutional Review Board Statement: Not applicable.

Informed Consent Statement: The human epidermis samples were obtained from waste material resulting from aesthetic surgical procedures, after obtaining patient consent for their use for research purposes. These materials were fully classifiable as non-identifiable biological materials, since they were handled throughout their preparation, transport, and storage in a manner that excludes any possibility of tracing sensitive patient data.

Data Availability Statement: Data will be provided on request.

Acknowledgments: We are indebted to Carlo Sirtori Foundation (Milan, Italy) for having provided part of equipment used in this experimentation. During the preparation of this work the authors used QuillBot tool for rephrasing. After using this tool, the authors reviewed and edited the content as needed and take full responsibility for the content of the publication.

Conflicts of Interest: The authors declare no conflicts of interest, except for patent WO2025114961A1, "Methods to counteract skin aging", owned by Università degli Studi di Milano, which is directly related to the content of this publication. The authors declare that patent WO2025114961A1, "Methods to counteract skin aging", has been licensed to Plantech s.r.l., a company in which C.L. is a scientific director and co-founder. The funders had no role in the design of the study; in the collection, analyses or interpretation of data; in the writing of the manuscript; or in the decision to publish the results R.P. reports no conflict of interest, he is a consultant in Plantech s.r.l. and not an employee.

Abbreviations

The following abbreviations are used in this manuscript:

AQP3	Aquaporin-3
BSA	Bovine serum albumin
CD	Circular dichroism
DMEM	Dulbecco's Modified Eagle's Medium
ECM	Extracellular matrix
ELISA	Enzyme-Linked Immunosorbent Assay
FBS	Fetal bovine serum
HA	Hyaluronic Acid
HAS2	Hyaluronan Synthase 2
HYAL1	Hyaluronidase 1
PBS	Phosphate-buffered saline
TFA	Trifluoroacetic acid

References

1. Negahdaripour, M.; Owji, H.; Eslami, M.; Zamani, M.; Vakili, B.; Sabetian, S.; Nezafat, N.; Ghasemi, Y. Selected Application of Peptide Molecules as Pharmaceutical Agents and in Cosmeceuticals. *Expert Opin. Biol. Ther.* **2019**, *19*, 1275–1287. [CrossRef]
2. Wang, L.; Wu, Z.; Wang, X.; Wang, X.; Mao, J.; Yan, Y.; Zhang, L.; Zhang, Z. Overview of Peptides and Their Potential Roles in Skin Health and Beauty. *J. Pept. Sci.* **2025**, *31*, e3668. [CrossRef]
3. Pintea, A.; Manea, A.; Pintea, C.; Vlad, R.-A.; Bîrsan, M.; Antonoaea, P.; Rédai, E.M.; Ciurba, A. Peptides: Emerging Candidates for the Prevention and Treatment of Skin Senescence: A Review. *Biomolecules* **2025**, *15*, 88. [CrossRef] [PubMed]
4. Bollati, C.; Fanzaga, M.; d'Adduzio, L.; Lammi, C. Molecular and Human In Vivo Study of an Innovative Plant-Derived Multifunctional Peptide Signaling the Collagen and Elastin Pathways and Melanin Production. *Cosmetics* **2025**, *12*, 100. [CrossRef]
5. Wong, F.-C.; Yong, A.-L.; Ting, E.P.-S.; Khoo, S.-C.; Ong, H.-C.; Chai, T.-T. Antioxidant, Metal Chelating, Anti-Glucosidase Activities and Phytochemical Analysis of Selected Tropical Medicinal Plants. *Iran. J. Pharm. Res.* **2014**, *13*, 1409–1415.
6. Yap, P.-G.; Gan, C.-Y. Multifunctional Tyrosinase Inhibitor Peptides with Copper Chelating, UV-Absorption and Antioxidant Activities: Kinetic and Docking Studies. *Foods* **2021**, *10*, 675. [CrossRef]
7. Musazzi, U.M.; Gennari, C.G.M.; Franzè, S.; Minghetti, P.; Cilurzo, F. Printing of Cutaneous Patches Loaded with Propranolol for the Treatment of Infantile Haemangiomas. *J. Drug Deliv. Sci. Technol.* **2021**, *66*, 102767. [CrossRef]
8. Jumper, J.; Evans, R.; Pritzel, A.; Green, T.; Figurnov, M.; Ronneberger, O.; Tunyasuvunakool, K.; Bates, R.; Žídek, A.; Potapenko, A.; et al. Highly Accurate Protein Structure Prediction with AlphaFold. *Nature* **2021**, *596*, 583–589. [CrossRef] [PubMed]
9. Baek, M.; DiMaio, F.; Anishchenko, I.; Dauparas, J.; Ovchinnikov, S.; Lee, G.R.; Wang, J.; Cong, Q.; Kinch, L.N.; Schaeffer, R.D.; et al. Accurate Prediction of Protein Structures and Interactions Using a Three-Track Neural Network. *Science* **2021**, *373*, 871–876. [CrossRef]
10. Lu, W.; Dong, C. Research Progress of Metal Chelating Peptides. *Food Health* **2022**, *4*, 19. [CrossRef]
11. Ngoc, L.T.N.; Moon, J.-Y.; Lee, Y.-C. Insights into Bioactive Peptides in Cosmetics. *Cosmetics* **2023**, *10*, 111. [CrossRef]
12. Ju, X.; Cheng, S.; Li, H.; Xu, X.; Wang, Z.; Du, M. Tyrosinase Inhibitory Effects of the Peptides from Fish Scale with the Metal Copper Ions Chelating Ability. *Food Chem.* **2022**, *390*, 133146. [CrossRef]
13. Godfrey, S.; Staite, W.; Bowtell, P.; Marsh, J. Metals in Female Scalp Hair Globally and Its Impact on Perceived Hair Health. *Int. J. Cosmet. Sci.* **2013**, *35*, 264–271. [CrossRef]
14. Cho, J. Jatrorrhizine Isolated from Phellodendron Amurense Improves Collagen Homeostasis in CCD-986sk Human Dermal Fibroblast Cells. *Cosmetics* **2025**, *12*, 70. [CrossRef]
15. Kirk, R.D.; Akanji, T.; Li, H.; Shen, J.; Allababidi, S.; Seeram, N.P.; Bertin, M.J.; Ma, H. Evaluations of Skin Permeability of Cannabidiol and Its Topical Formulations by Skin Membrane-Based Parallel Artificial Membrane Permeability Assay and Franz Cell Diffusion Assay. *Med. Cannabis Cannabinoids* **2022**, *5*, 129–137. [CrossRef]
16. Parker, J.L.; Deme, J.C.; Wu, Z.; Kuteyi, G.; Huo, J.; Owens, R.J.; Biggin, P.C.; Lea, S.M.; Newstead, S. Cryo-EM Structure of PepT2 Reveals Structural Basis for Proton-Coupled Peptide and Prodrug Transport in Mammals. *Sci. Adv.* **2021**, *7*, eabh3355. [CrossRef] [PubMed]
17. Verdier-Sévrain, S.; Bonté, F. Skin Hydration: A Review on Its Molecular Mechanisms. *J. Cosmet. Dermatol.* **2007**, *6*, 75–82. [CrossRef]

18. Reilly, D.M.; Lozano, J. Skin Collagen through the Lifestages: Importance for Skin Health and Beauty. *Plast. Aesthet. Res.* **2021**, *8*, 2. [CrossRef]
19. Naidoo, K.; Birch-Machin, M. Oxidative Stress and Ageing: The Influence of Environmental Pollution, Sunlight and Diet on Skin. *Cosmetics* **2017**, *4*, 4. [CrossRef]
20. Abatangelo, G.; Vindigni, V.; Avruscio, G.; Pandis, L.; Brun, P. Hyaluronic Acid: Redefining Its Role. *Cells* **2020**, *9*, 1743. [CrossRef]
21. Aguilar-Toalá, J.E.; Hernández-Mendoza, A.; González-Córdova, A.F.; Vallejo-Cordoba, B.; Liceaga, A.M. Potential Role of Natural Bioactive Peptides for Development of Cosmeceutical Skin Products. *Peptides* **2019**, *122*, 170170. [CrossRef]
22. Waszkielewicz, A.M.; Mirosław, K. Peptides and Their Mechanisms of Action in the Skin. *Appl. Sci.* **2024**, *14*, 11495. [CrossRef]
23. Badilli, U.; Inal, O. Current Approaches in Cosmeceuticals: Peptides, Biotics and Marine Biopolymers. *Polymers* **2025**, *17*, 798. [CrossRef]
24. Robinson, L.R.; Fitzgerald, N.C.; Doughty, D.G.; Dawes, N.C.; Berge, C.A.; Bissett, D.L. Topical Palmitoyl Pentapeptide Provides Improvement in Photoaged Human Facial Skin [1]. *Int. J. Cosmet. Sci.* **2005**, *27*, 155–160. [CrossRef]
25. Puig, A.; Antón, J.M.G.; Mangues, M. A New Decorin-like Tetrapeptide for Optimal Organization of Collagen Fibres. *Int. J. Cosmet. Sci.* **2008**, *30*, 97–104. [CrossRef] [PubMed]
26. Gorouhi, F.; Maibach, H.I. Role of Topical Peptides in Preventing or Treating Aged Skin. *Int. J. Cosmet. Sci.* **2009**, *31*, 327–345. [CrossRef] [PubMed]
27. Pickart, L.; Margolina, A. Skin Regenerative and Anti-Cancer Actions of Copper Peptides. *Cosmetics* **2018**, *5*, 29. [CrossRef]
28. Jiang, F.; Wu, Y.; Liu, Z.; Hong, M.; Huang, Y. Synergy of GHK-Cu and Hyaluronic Acid on Collagen IV Upregulation via Fibroblast and Ex-vivo Skin Tests. *J. Cosmet. Dermatol.* **2023**, *22*, 2598–2604. [CrossRef] [PubMed]
29. Hussain, M.; Goldberg, D.J. Topical Manganese Peptide in the Treatment of Photodamaged Skin. *J. Cosmet. Laser Ther.* **2007**, *9*, 232–236. [CrossRef]
30. Dana, A.; Rotsztejn, H. The Peptide Argireline-The Importance of Local Application on the Skin, in the Light of Current Knowledge. *Lett. Drug Des. Discov.* **2017**, *14*, 1215–1220. [CrossRef]
31. Surbek, M.; Sukseree, S.; Eckhart, L. Iron Metabolism of the Skin: Recycling versus Release. *Metabolites* **2023**, *13*, 1005. [CrossRef]
32. Pretzler, M.; Rompel, A. Tyrosinases: A Family of Copper-Containing Metalloenzymes. *ChemTexts* **2024**, *10*, 12. [CrossRef]
33. Bang, J.; Hwang, Y.-L.; Kim, M.Y.; Yun, J.N.; Hyun, E.; Chang, M.Y.; Shin, D.H.; Kim, S.; Lee, J.-H. Wrinkle-Improving Effect of Novel Peptide That Binds to Nicotinic Acetylcholine Receptor. *Int. J. Mol. Sci.* **2024**, *25*, 7860. [CrossRef]
34. Sim, G.S.; Lee, D.-H.; Kim, J.-H.; An, S.-K.; Choe, T.-B.; Kwon, T.-J.; Pyo, H.-B.; Lee, B.-C. Black Rice (*Oryza sativa* L. Var. *japonica*) Hydrolyzed Peptides Induce Expression of Hyaluronan Synthase 2 Gene in HaCaT Keratinocytes. *J. Microbiol. Biotechnol.* **2007**, *17*, 271–279. [PubMed]
35. Zonari, A.; Brace, L.E.; Li, F.; Harder, N.H.O.; Harker, C.; Jacob, C.; Kaufman, J.; Chilukuri, S.; Oliveira, C.R.; Boroni, M.; et al. Clinical Efficacy of OS-01 Peptide Formulation in Reducing the Signs of Periorbital Skin Aging. *Int. J. Cosmet. Sci.* **2025**, *47*, 455–465. [CrossRef] [PubMed]
36. Norzagaray-Valenzuela, C.D.; Valdez-Ortiz, A.; Shelton, L.M.; Jiménez-Edeza, M.; Rivera-López, J.; Valdez-Flores, M.A.; Germán-Báez, L.J. Residual Biomasses and Protein Hydrolysates of Three Green Microalgae Species Exhibit Antioxidant and Anti-Aging Activity. *J. Appl. Phycol.* **2017**, *29*, 189–198. [CrossRef]
37. Kim, H.; Jeon, B.; Lee, H.-J.; Chung, D.-K. Evaluation of the Skin Moisturizing Efficacy of a Collagen Peptide Isolated from Fish Scales, Using HaCaT Keratinocytes. *J. Korean Soc. Food Sci. Nutr.* **2020**, *49*, 454–461. [CrossRef]
38. Baker, P.; Huang, C.; Radi, R.; Moll, S.B.; Jules, E.; Arbiser, J.L. Skin Barrier Function: The Interplay of Physical, Chemical, and Immunologic Properties. *Cells* **2023**, *12*, 2745. [CrossRef]
39. Kudo, M.; Katayoshi, T.; Kobayashi-Nakamura, K.; Akagawa, M.; Tsuji-Naito, K. H+/Peptide Transporter (PEPT2) Is Expressed in Human Epidermal Keratinocytes and Is Involved in Skin Oligopeptide Transport. *Biochem. Biophys. Res. Commun.* **2016**, *475*, 335–341. [CrossRef]

Disclaimer/Publisher's Note: The statements, opinions and data contained in all publications are solely those of the individual author(s) and contributor(s) and not of MDPI and/or the editor(s). MDPI and/or the editor(s) disclaim responsibility for any injury to people or property resulting from any ideas, methods, instructions or products referred to in the content.